Supplementary Information for "Multiscale Generalized Network Model Using Differential Micro-CT Imaging for Drainage in Heterogeneous Carbonates"

Asli S. Gundogar[a,b*], Sajjad Foroughi[a], Aninditya Patmonoaji[a,c], Mohamed Regaieg[d], Martin J. Blunt[a], Branko Bijeljic[a]

[a]Department of Earth Science and Engineering, Imperial College London, London, SW7 2AZ, United Kingdom
[b]Department of Petroleum and Natural Gas Engineering, Middle East Technical University, Ankara, 06800, Turkey
[c]Department of Chemical Engineering, University College London, London, WC1E 6BT, UK
[d]TotalEnergies, OneTech, Pau, 64000, France

*Corresponding author.

Contents of this file

This Supplementary Information provides additional figures that complement the main manuscript.

1. Figures S1 to S6

Introduction

Figures S1 to S3 illustrate the improvements in the Generalized Network Model (GNM) related to corner connectivity. Figures S4 and S6 show the drainage capillary pressure and relative permeability results for the µCT-resolved (macro-) networks of the Ketton(II) and reservoir carbonate samples, respectively. Figure S5 shows µCT slices for each subvolume (SV) of the reservoir carbonate sample.

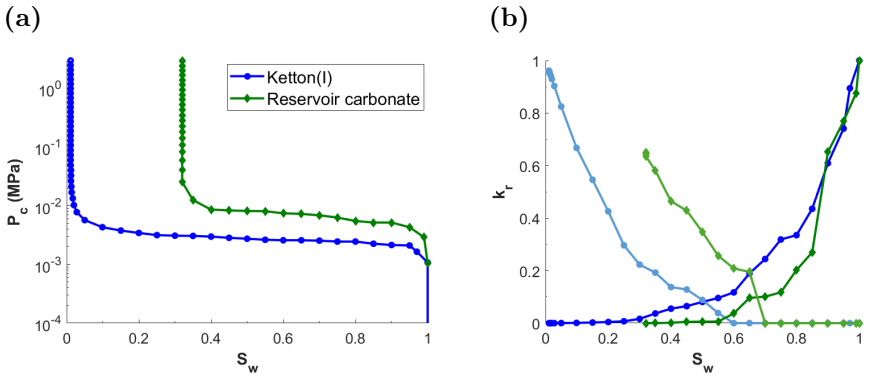

Fig. S1: Comparison of drainage capillary pressure and relative permeability for the µCT-resolved networks of Ketton(I) and reservoir carbonate SV1 prior to corner connectivity enhancement, excluding the effects of unresolved porosity.

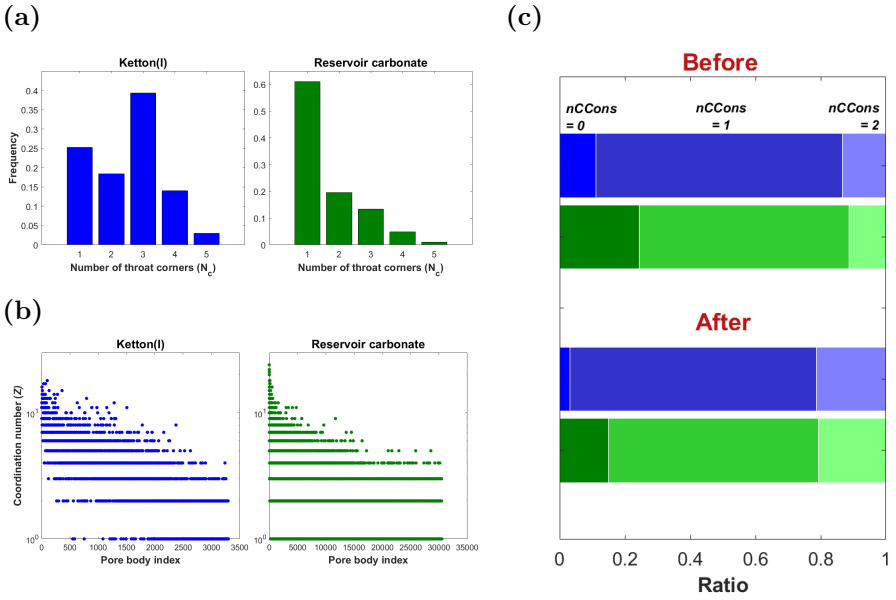

Fig. S2: Comparison of the µCT-resolved network properties for the Ketton(I) and reservoir carbonate SV1s, shown in blue and green, respectively: (a) histogram of number of throat corners (N_c) ; (b) coordination number (Z) distribution; and (c) histogram of number of corner connectivity ($nCCons$).

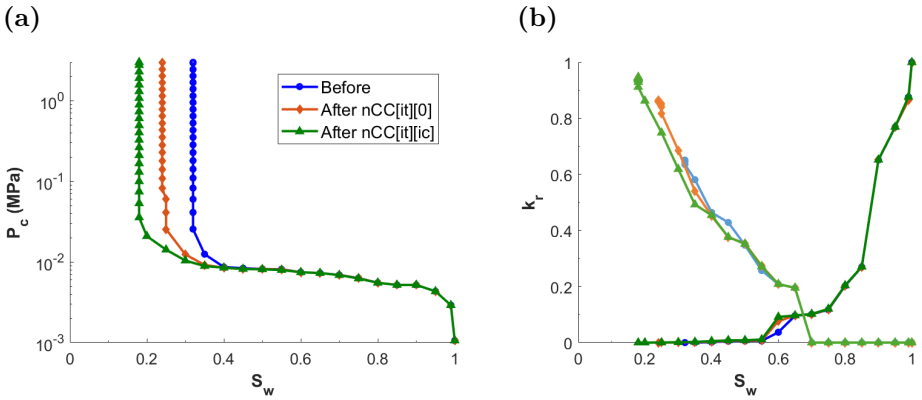

Fig. S3: Drainage capillary pressure (a) and relative permeability (b) for the µCT-resolved network of the reservoir carbonate, showing the impact of enhanced corner connectivity (from blue to dark green). The 2D vector $nCCons$ indexes the throat it and specifies the order of corners (ic) within that throat. Results in (a) and (b) show a gradual decrease in S_{wi} and an increase in endpoint k_{ro} with improved corner connectivity, respectively.

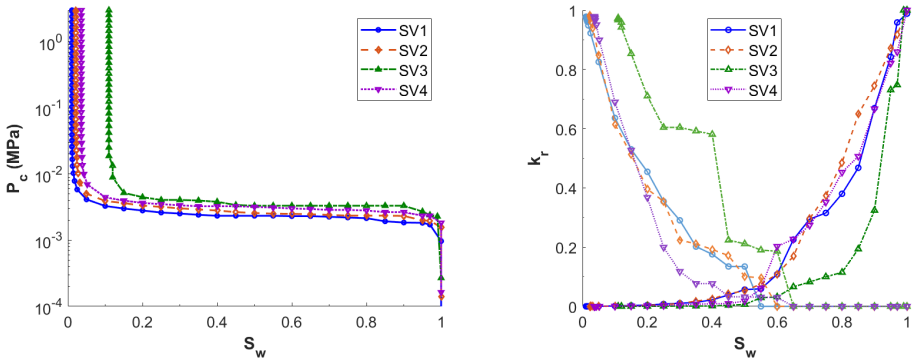

Fig. S4: Drainage capillary pressure (a) and relative permeability (b) for the µCT-resolved networks of Ketton(II) subvolumes (SVs) after corner connectivity enhancement, excluding the effects of unresolved porosity.

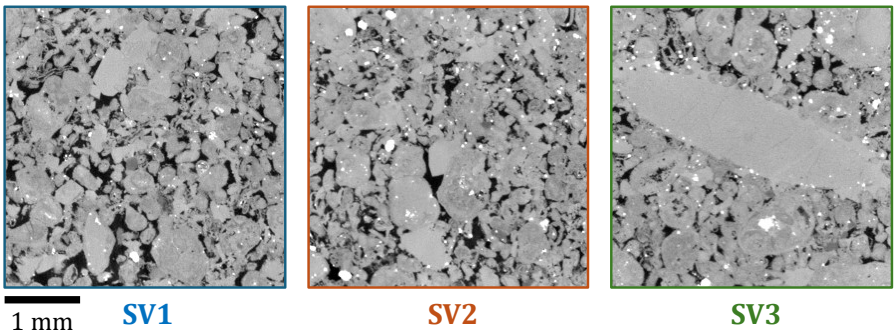

Fig. S5: Representative cross-sectional slices from three subvolumes of the reservoir carbonate, demonstrating the progressive increase in pore-space heterogeneity from SV1 to SV3.

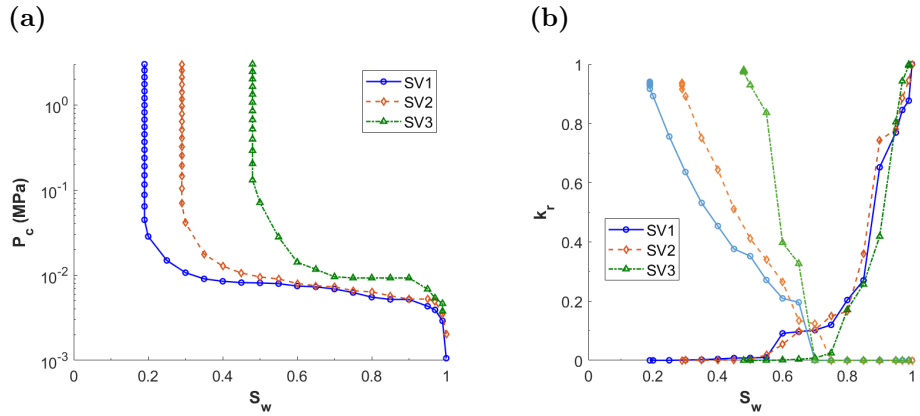

Fig. S6: Drainage capillary pressure (a) and relative permeability (b) for the µCT-resolved networks of reservoir carbonate subvolumes (SVs) after corner connectivity enhancement, excluding the effects of unresolved porosity.